J Mater Sci: Mater Med (2011) 22:829–838
DOI 10.1007/s10856-011-4270-2

Influence of calcinated and non calcinated nanobioglass particles on hardness and bioactivity of sol–gel-derived TiO_2–SiO_2 nano composite coatings on stainless steel substrates

Mohammad Saleh Dadash · Saeed Karbasi · Mojtaba Nasr Esfahani · Mohammad Reza Ebrahimi · Hojatollah Vali

Received: 5 January 2010 / Accepted: 20 February 2011 / Published online: 6 March 2011

Abstract Thick films of calcinated and non calcinated nanobioglass (NBG)-titania composite coatings were prepared on stainless steel substrates by alkoxide sol–gel process. Dip-coating method was used for the films preparation. The morphology, structure and composition of the nano composite films were evaluated using environmental scanning electron microscope, X-ray diffraction and Fourier transform infrared spectroscope. The SEM investigation results showed that prepared thick NBG-titania films are smooth and free of macrocracking, fracture or flaking. The grain size of these films was uniform and nano scale (50–60 nm) which confirmed with TEM. Also FTIR confirmed the presence of Si–O–Si bands on the calcinated NBG-titania films. The hardness of the prepared films (TiO_2-calcinated NBG and TiO_2-Non calcinated NBG) was compared by using micro hardness test method. The results verified that the presence of calcinated NBG particles in NBG-titania composite enhanced gradually the mechanical data of the prepared films. The in vitro bioactivity of these films was discussed based on the analysis of the variations of Ca and P concentrations in the simulated body fluid (SBF) and their surface morphologies against immersion time. Surface morphology and Si–O–Si bands were found to be of great importance with respect to the bioactivity of the studied films. The results showed that calcinated NBG-titania films have better bioactivity than non calcinated NBG-titania films.

M. S. Dadash · M. N. Esfahani · M. R. Ebrahimi
Department of Material Engineering, Islamic Azad University-Najafabad Branch, Isfahan, Iran

S. Karbasi (✉)
Medical Physics and Biomedical Engineering Group, Department of Medicine, Isfahan University of Medical Sciences, Isfahan, Iran
e-mail: karbasi@med.mui.ac.ir

H. Vali
McGill Institute for Advanced Materials, McGill University, Montreal, QC H3A 2B2, Canada

1 Introduction

In 1971, Hench reported on the discovery that certain compositions of silicate glasses can form a bond with bone tissue [1]. Research has shown that these bioactive glasses can also bond with certain types of connective tissue through attachment of collagen to the glass surface [2].Beginning in 1985, bioactive glasses and glass–ceramics have been used in a number of clinical applications, and their use has increased steadily over the recent years [3–9]. The bonding of these bioactive glasses and glass—ceramics to bone has been attributed to a series of surface reactions that occur when the material is implanted [10–20].

Certain compositions of bioactive glasses containing SiO_2–CaO–P_2O_5 bond to both soft and hard tissue without an intervening fibrous layer. Results of in vivo implantation showed that these compositions produce no local or systemic toxicity, no inflammation, and no foreign-body response [21]. Bioactive glasses present critical drawbacks in their low mechanical properties and this causes great limitations to their use for load bearing sites.

It is obvious that low mechanical properties will cause some revision surgeries in patient. These revision surgeries which cause pain for the patient, are very expensive and also their success rate is rather small. For this reason, bioglass parts often coupled with a tough material, providing thus their excellent surface properties without a great loss in the bioactivity of the bioactive glass [22].

Titania film is a well-known material that used in a wide variety of applications and especially in medical applications. Titania nano film has very excellent corrosion resistance, hardness and wear resistance [23]. In addition, sol–gel derived titania coatings have been described to be apatite nucleation inducers not only in vitro but also in vivo [24]. It has been proposed that the nucleation of the calcium phosphate is activated by the presence of hydroxyl functional groups in the film [25]. Descriptions concerning thickness and morphology effects on the nucleation ability of these films have been reported [26].

Titania films introduced on a metal surface by various techniques, like sol–gel technique [27–30]. The sol–gel process is a method for preparing inorganic oxide ceramics from colloidal and polymeric sols. The temperatures are significantly lower than those in traditional processing methods. The potential advantages of thin sol–gel derived coatings over other bioactive glass, glass–ceramic and ceramic coatings are addressed to the simpler production processes, thinner coatings and reduced dissolution rates (chemically durable). The possibility of modifying the surface area, porosity, composition, adsorption capacity, dissolution rate and the subtility in producing coatings as well as bulk materials make the use of sol–gel derived materials very attractive in the field of medicine and dentistry. Possible uses of these materials are as biodegradable, protective, optical and medical coatings, fillers, membranes, sensors and cell growth substrates. Films can be produced for instance by spin and dip coating. Uniform thin coatings can be deposited by dip coating onto substrates of large dimensions and complex geometries [31, 32]. Therefore, titania could be a good coupled material for bioglass to optimized the composite properties.

The present work is concerned with the preparation and characterization of a novel biocomposite containing Nano bioactive glass (NBG) and titania. To our knowledge, no special study reported the influence of calcinated and non calcinated bioactive glass particles on mechanical properties and bioactivity of the composite films. This work aims to demonstrate these effects.

2 Materials and method

2.1 Materials

Starting materials used in this preparation were analytical grade Tetraethyl orthosilicate (TEOS, Merck), Triethyl phosphate (TEP, Merck), $Ca(NO_3)_2{\cdot}4H_2O$ (Merck), ammonia (Merk), nitric acid (Merck), Commercial extra pure titanium isopropoxide (TTIP, Merk), isopropanol (iPrOH, Merck), Diethanolamine (DEA, Merck). All materials were used as received without further purification.

2.2 Preparation of nano-bioactive-glasses (NBG)

NBG was prepared by an alkali-mediated sol–gel method. In a typical preparation of nano-bioactive 58S glass [33–35] (SiO_2:CaO:P_2O_5 = 58:23:9, weight ratio), TEOS (21.6 ml), distilled water (13.9 ml) and 2 M HNO_3 (2.8 ml) were dissolved in ethanol (50 ml) and stirred at room temperature for 30 min. TEP (2.2 ml) was then dissolved into the prepared acid silica sol. After stirring for 20 min, the $Ca(NO_3)_2{\cdot}4H_2O$ (14.04 g) was added into the acid sol. A certain concentration (2.0 mol/l) of ammonia solution (10 ml) was dropped into the acid sol while vigorously stirring after $Ca(NO_3)_2{\cdot}4H_2O$ was completely dissolved. The sol swiftly gelated. The obtained gel was stirred by magnet in order to avoid forming bulk gel and then the resulting gel was kept in the oven at 60°C for 1 day to remove the residual water and ethanol. The dry gel powders were calcinated at 600°C in air for 2 h. The heating rate of calcinations was fixed at 3°C/min. The glass composition was analyzed by X-ray Fluorescence method (PW2404, PHILIPS). The analyzing result (Table 1) showed that the composition of obtained glass was almost consistent with the designed composition.

2.3 Preparation of Titania sol

A 0.5 M solution of TTIP (7.5 ml) in iPrOH (47.9 ml) was prepared and subsequently a suitable amount of DEA (9.15 ml) was added to the solution. A molar ratio of DEA/TTIP = 4 was used. The solution was stirred at room temperature for 2 h. Subsequently water (0.86 g) was added drop by drop under vigorous stirring. A molar ratio of H_2O/TTIP = 2 was used. A clear sol was obtained. This Sol was stable at room temperature and no changes were observed even after storage for many months.

2.4 Preparation of nanostructured bioactive glass-Titania composite coating

The nanostructured bioactive glass-Titania composite was prepared by addition of 70 g/l of calcinated and non calcinated NBG powders to prepared Titania sol. As discussed the powder was added slowly under vigorous stirring to prevent the formation of agglomerates. A thick, white, viscous solution was obtained. This solution settled slowly over a period of 2 weeks. To prevent settling the modified

Table 1 The bioactive glass composition (weight ratio, %)

	SiO_2	CaO	P_2O_5	Impurity
Design	58	33	9	0.07
Experiment	58.39	34.5	6.5	

sol was stirred constantly while in storage between experiments. The stainless steel substrates 316 L (with 15 mm diameter) to be coated were cleaned with ethanol and then washed ultrasonically in distilled water. This cycle was repeated five times and then substrates were dried at 125°C for 4 h. Two stainless steel disks of 15 mm diameter were placed in two beakers. The sol container was kept at 0°C in order to slow down the condensation reaction. The beakers with the stainless steel filled with the composite sol (one with calcinated NBG powder and other with non calcinated NBG) and the films were deposited on stainless steel substrates by dip coating with withdrawal speed of 0.30 mm/s.Subsequently the deposite films were dried in air at room temperature for 24 h and then heat-treated. After heat treatment and cooling, the disks were removed and put back in the beaker prior to coating again. This cycle was repeated two times. Heat treatment for all samples was done using a multi-segment programmable furnace (Exciton 1500). The furnace temperature was increased at a ramp rate of 3°C per minute until it reached 100°C and was held at 100°C for 1 h. Subsequently, the temperature was increased at a ramp rate of 3°C to 600°C and held for 1 h in this temperature. Finally the furnace was allowed to cool down naturally to room temperature. The cooling down period took approximately 12 h.

2.5 Characterization of nano-composite coating

The microstructure of NBG powder was investigated using Hitachi600 transmission electron microscope. Scanning electron microscope (Phillips XL 30) was used to determine the thickness and morphology of nanostructure composite films on substrates. The same instrument was also used to perform electron diffraction spectroscopy (EDS) quantitative analysis of nanostructure composite films. The prepared films were characterized by Philips X'pert MPD diffractometer using Cu Kα generated at 40 kV and 40 mA. The samples were scanned from 10° to 90° with a step size of 0.02° and a count rate of 3.0°/min. The film surfaces were analyzed using Fourier transform infrared spectroscopy (Bomem, MB-100) in diffuse reflectance mode.

2.6 Hardness tests

The hardness of the films obtained by two dip coating/heat treatment cycles was determined with a Vickers microhardness measuring device (FischerScope HM2000 S) as described in DIN EN ISO 14577. The reported values are averages of ten measurements performed on different locations in the center section of each sample. The thickness of all coatings is more than ten times, the maximum indentation depth of 1 μm in order to reduce effects of the substrates.

2.7 In vitro bioactivity

The bioactivity of the coatings was studied by immersing the coatings in 22 mL of simulated body fluid (SBF) [36] at 37°C for up to 4 weeks. SBF was prepared by dissolving reagent chemicals of NaCl, $NaHCO_3$, KCl, $K_2HPO_4{\cdot}3H_2O$, $MgCl_2{\cdot}6H_2O$, $CaCl_2{\cdot}2H_2O$ and Na_2SO_4 into deionized water. The solution was buffered at physiological pH 7.40 at 37°C with hydrochloric acid (2 M HCl). The ion concentrations of SBF (Na^+ 142.0, K^+ 5.0, Mg^{2+} 1.5, Ca^{2+} 2.5, Cl^- 147.8, HCO_3^- 4.2, HPO_4^{2-} 1.0, SO_4^{2-} 0.5 mM) are nearly equal to that of human plasma. Two coatings (calcinated and non calcinated NBG-titania films) were immersed in closed polyethylene tubes and the tubes were placed in a shaking water bath having a constant temperature at 37°C. After immersion the coatings were removed from the fluid, gently rinsed with distilled water and dried at 40°C before surface analysis. The formation of the apatite layer on the coatings were recognized, analyzed and confirmed using Scanning electron microscopy (SEM) and energy dispersive spectroscopy (EDS) techniques (Phillips XL 30).

3 Results and discussion

3.1 NBG powder characterization

TEM images revealed that the NBG particles are spheredshape with uniform morphology. The particles have an average size of approximately 50–60 nm which is suitable for cell attachment (Fig. 1) [37, 38]. According to the literatures, the cell response enhance in the presence of ceramic nanoparticles less than 100 nm in diameter [37]. The enhanced cell response may result from the prerequisite protein adsorption, which is also influenced by the nanodimensions [37]. TEM Energy dispersive spectroscopy (EDS) of calcinated NBG powders showing the presence of Ca and Si and O in the samples. The Cu signal is from the TEM grid. The XRD study confirmed that the calcinated and non calcinated glass generally existed in amorphous state as no diffraction peaks could be observed except a broad band between 15° and 40° (2θ) (Fig. 2).

3.2 Nano composite characterization

Figure 3 shows the XRD patterns of NBG-titania films. Diffractograms confirm the formation of anatase phase in both calcinated and non calcinated NBG-titania films on stainless steel substrates. They are also indicating that as

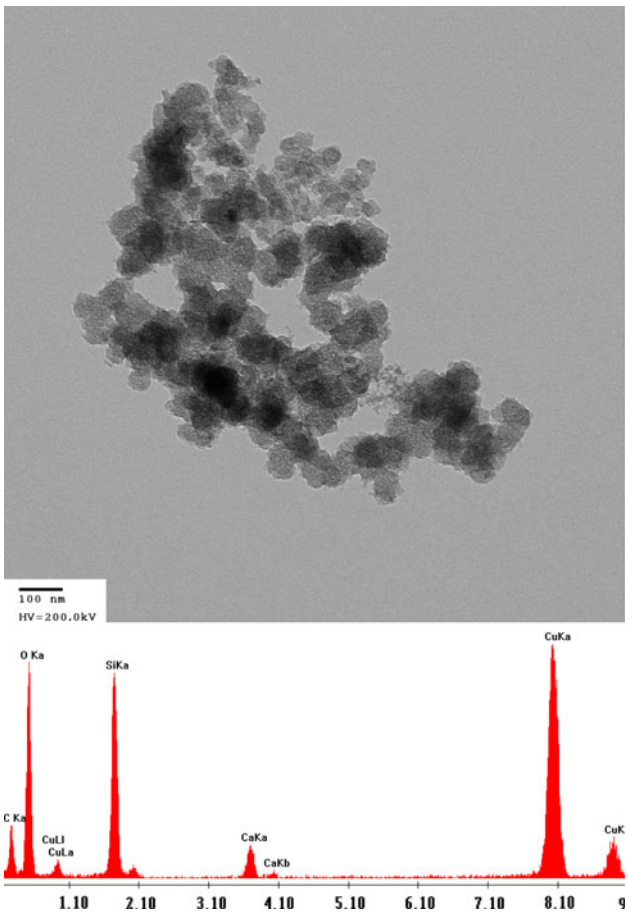

Fig. 1 TEM image of NBG particles with energy dispersive spectroscopy (EDS) of calcinated NBG powders

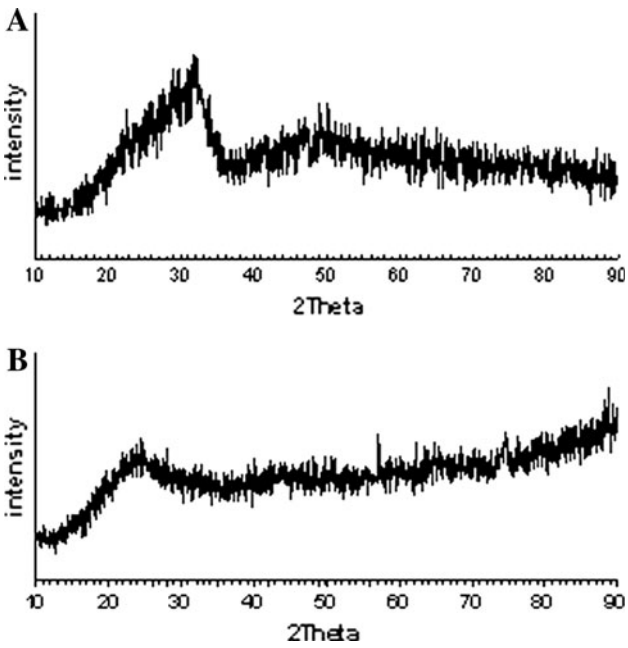

Fig. 2 X-ray diffractogram for (**a**) Calcinated, (**b**) Non calcinated NBG particles

the number of coating increase, the amount of anatase increase as is evident from the peaks.

Titania exists mainly in three polymorphs: rutile, anatase and brookite. Rutile is considered as the stable form of titania. Anatase is metastable and converts to rutile at high temperatures accompanying grain growth. It has been suggested that titania has different properties depending on its micro-structure. Compared to rutile titania, anatase titania has unique properties and advantages for medical applications. Anatase exhibits stronger interactions with metal compared to rutile, and the surface of anatase titania can absorb more OH^- and PO_4^{3-} than that of rutile titania in body fluid, which is in favor of depositing bone-like apatite [39, 40].

The FTIR test results from the calcinated and non calcinated nanobioglass (NBG)-Titania films are obtained in Fig. 4. It is reported that the high-frequency part of the spectra is dominated by the OH stretching vibration (3,500–3,900 cm^{-1}) and bending vibration (1400–1640 cm^{-1}) of water. The peaks at about, 600–700 cm^{-1}, 1,110 cm^{-1} are correspond to Ti, Ti–O and unsymmetry stretching vibration of Si–O–Si, respectively. Two absorption bands near 1,036 cm^{-1} and 930–970 cm^{-1} can be ascribed to the stretching vibration of Ti–O–Si, respectively [41–43]. The above results confirmed the presence of Si–O–Si bands in calcinated NBG-titania films. In vitro studies have shown that the nucleation and crystallization rates of hydroxycarbonate apatite (HCA) depend on many factors including the sol–gel prepared film composition [44, 45], their textural properties (surface area and porosity) [46], as well as changes in the ionic composition of the assay solution [47].

In bone environment, additional advantage can be obtained by releasing silica, which has been shown to activate bone forming cells resulting in enhanced bone growth [48]. In addition, calcium phosphate was able to nucleate on the coatings which have Si–O–Si bands on their surface. So it can be concluded that calcinated NBG-titania films could have better bioactivity than non calcinated NBG-titania films due to presence of Si–O–Si bands on their surface.

SEM morphologies of prepared films coated on stainless steel substrate are shown in Fig. 5. The bioglass nanoparticles are embedded in the matrix of the Titania gel (Fig. 6). The morphology appears rough and homogeneous, with some submicron pores and cracks due to small residual compressive stresses [49].The extent and frequency of the micro cracks increase with the number of dip coating/heat treatment cycles. These stresses are caused by chemical reactions during drying and also difference in thermal expansion coefficients between substrate and the TiO_2 films. The observed absence of macro cracking may be explained by the competitive action of three stresses.

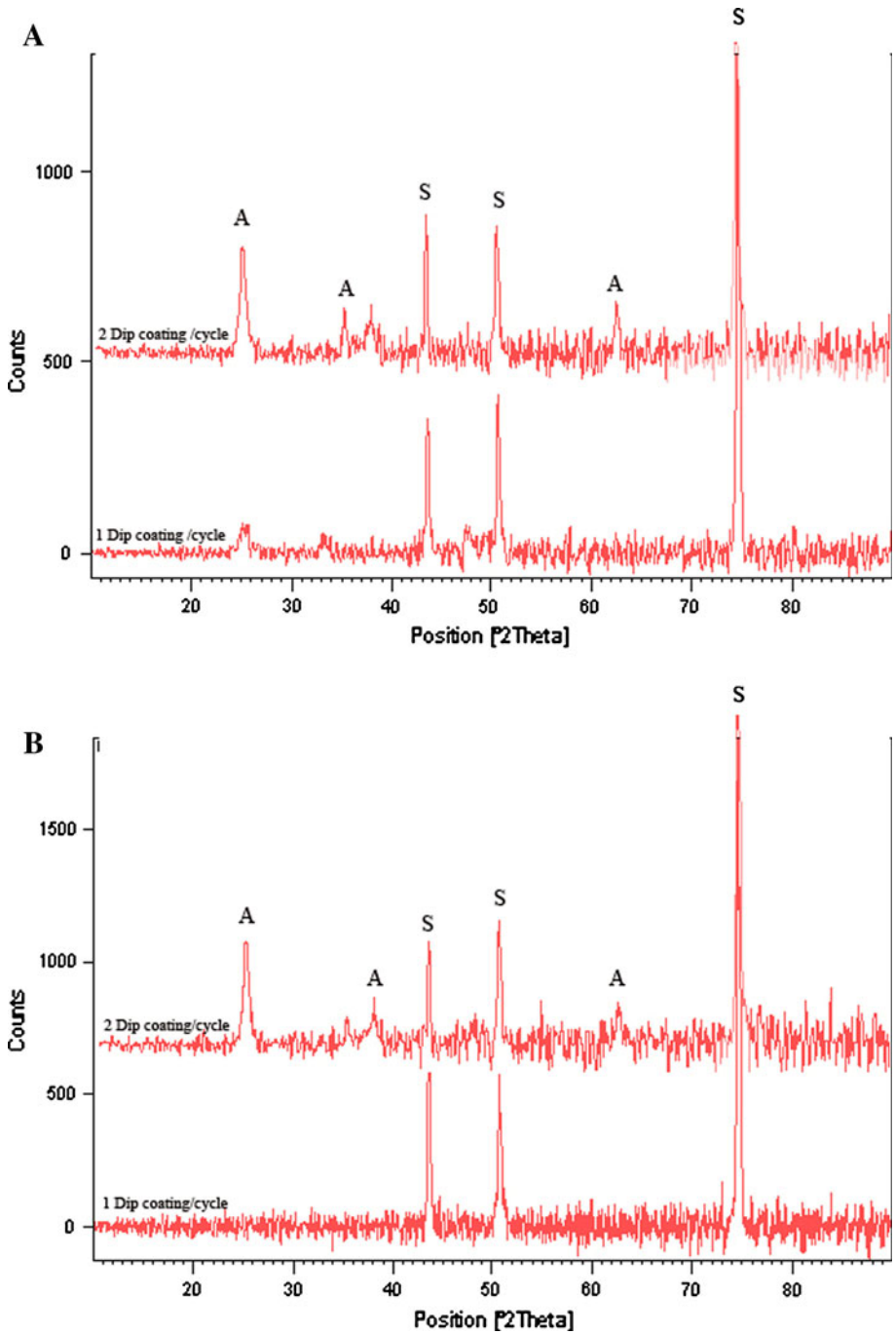

Fig. 3 X-ray diffractogram for stainless steel substrates coated two times with (**a**) Calcinated NBG-titania nano composite sol (**b**) Non calcinated NBG-titania nano composite sol and heat treated at 600°C. (*A* Anatase, *S* substrate)

When crystallization occurs, large compressive stresses are generated [50]. When grain growth and densification of the film occurs, the stresses are reduced [51]. The densification that accompanies grain formation is directly proportional to grain size [51].Since the nanobioglass particles provide an initial grain growth site ($\approx$30 nm), the growth takes place fairly quickly and, consequently, the compressive stresses are reduced quickly. Also the stainless steel substrate has a higher coefficient (17×10^{-6}°C) of linear thermal expansion than the TiO_2 films ($2.1–2.8 \times 10^{-6}$°C) [52]. On cooling, the stainless steel substrate shrinks more than the TiO_2 films leading to further reduction of compressive stresses and these reduced compressive stresses lead to the formation of small micro cracks.

In our investigation we have also found that a porous morphology appears in calcinated NBG-titania films (Fig. 7). The thickness of the films obtained per two dip coating/heat treatment cycles from the calcinated and non

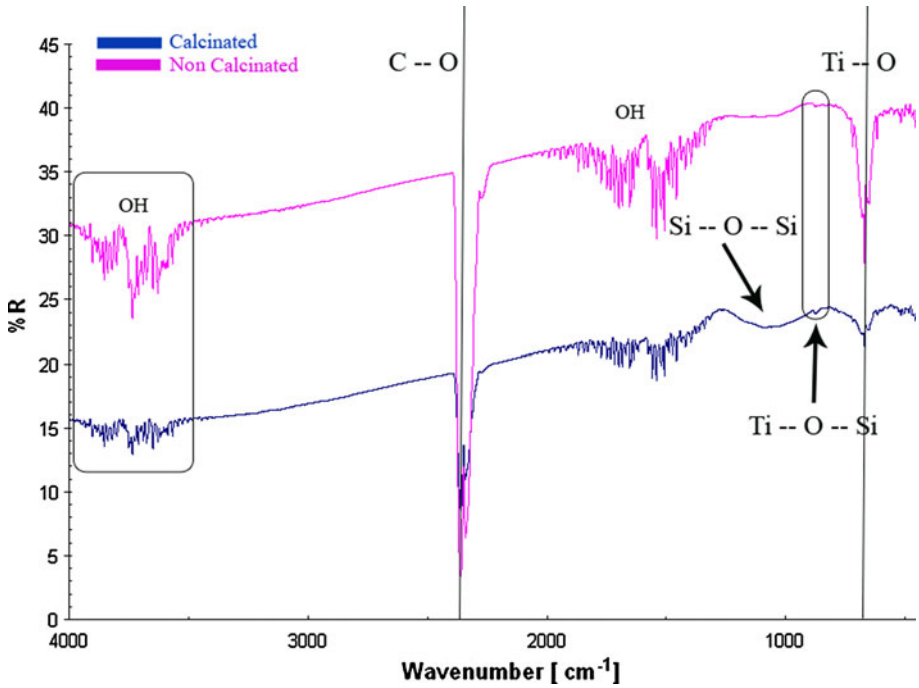

Fig. 4 FTIR spectra of calcinated and non calcinated NBG-titania films

calcinated nanobioglass (NBG)-titania films are obtained in Fig. 8. It can be concluded that the films obtained from calcinated NBG particles (303.70 μm) are thicker than those obtained from non calcinated NBG particles (245.20 μm) due to higher adhesive properties.

The bulk compositions of the coatings obtained by EDS analysis confirmed the Ca, Si, P and Ti presents in both calcinated and non calcinated NBG-titania films (Fig. 9). It is obvious that elemental values for calcinated NBG-titania film are significantly higher than those values obtained from non calcinated NBG-titania film.

3.3 Hardness tests

Table 2 presents the Vickers hardness values of NBG-titania films. The average value of ten measurements at different places on the films was recorded. The obtained values clearly indicates that calcinated NBG-titania films have a higher hardness than non calcinated NBG-titania films due to dense structure and morphology of calcinated NBG-titania films (Fig. 10). On the same grounds, it can be assumed that increasing the bond strength of the ionic link in calcinated NBG particles is expected to strengthen the glass structure and consequently increases the Vicker's hardness [53]. The Vickers micro hardness for some biomedical materials is shown in Table 3. It is obvious that mechanical properties of Sol–gel derived Bioglass 58S enhanced by the high hardness and strength of the Titania matrix.

3.4 Bioactivity measurement

SEM images of calcinated and non calcinated NBG-titania films before soaking show a rough and homogeneous surface with some submicron pores and cracks (Fig. 5). After immersion in SBF for 30 days, a layer of numerous sphered-like particles appeared, covering the films surface. Moreover, electron diffraction spectroscopy analyses (EDS) reveal that those particles are calcium-phosphate crystals (Fig. 11).

Figure 12 shows the surface morphology of NBG-titania films after immersing in SBF for 30 days.Calcinated NBG-titania films, Due to high porosity in composite film and also presents of Si–O-Si bands on their surface, can facilitate rapid and massive release of Ca^{2+} ions from the film into the solution. This rapid release increases the Ca^{2+} saturation and facilitates the formation of nucleation sites (Si–OH), and induces rapid deposition of apatite on the surface. The crystallization of insoluble HCA is believed to involve in the formation of meta-stable CaP phases. HCA is the least soluble phase at pH = 7.4 and, in the absence of kinetic complications, it should be thermodynamically the most stable species [54]. In the opposite side we have non calcinated NBG-titania films. In these films even after soaking for 30 days, only a few signs of formation of sphere-like apatite can be found on the surface.

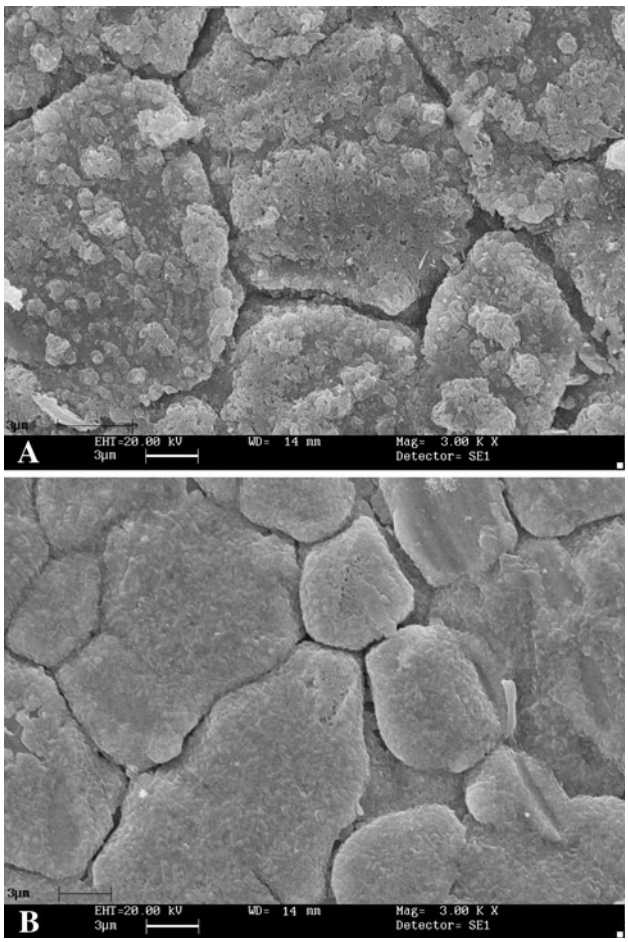

Fig. 5 SEM micrograph of stainless steel coated with (**a**) calcinated NBG-titania sol and (**b**) Non calcinated NBG-titania sol after two dip coating/heat treatment cycles at 600°C. morphology appears rough and homogeneous, with some submicron pores and cracks

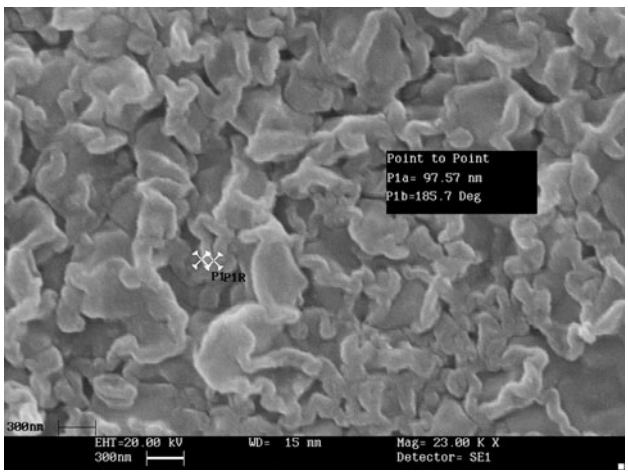

Fig. 6 The bioglass nano particles in the matrix of the Titania gel. It is obvious that the particle sizes are less than 100 nm

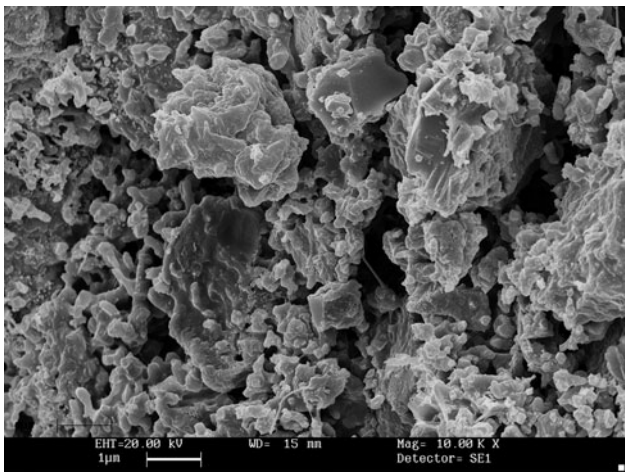

Fig. 7 Scanning electron micrograph of high porosity and pore volume in calcinated NBG-titania films

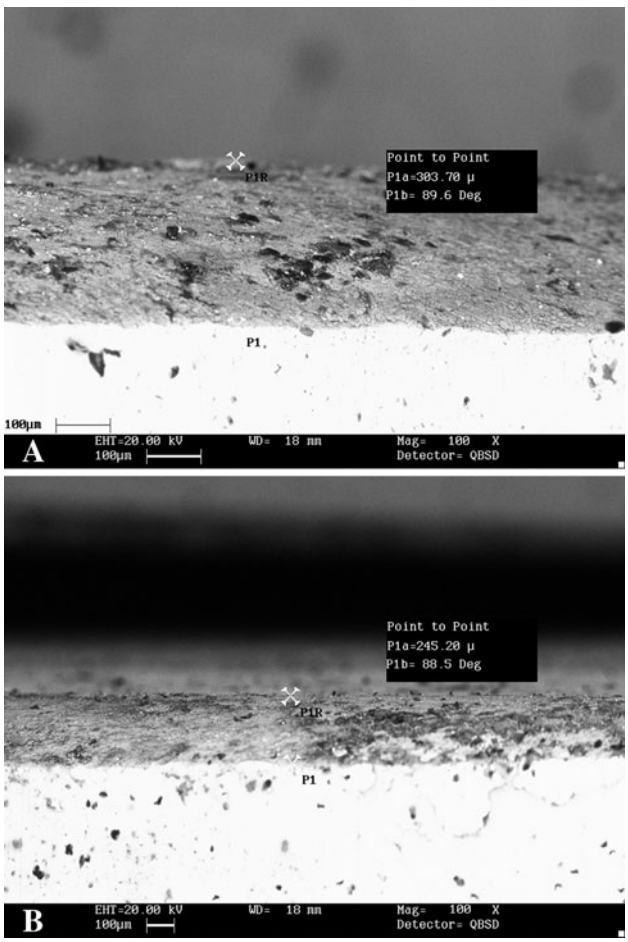

Fig. 8 The thickness of the films obtained per two dip coating/heat treatment cycles from (**a**) calcinated and (**b**) Non calcinated NBG-Titania films. The unfocused zone [indicated with *arrow sign* in part B] is obtained due to incline position of sample in SEM

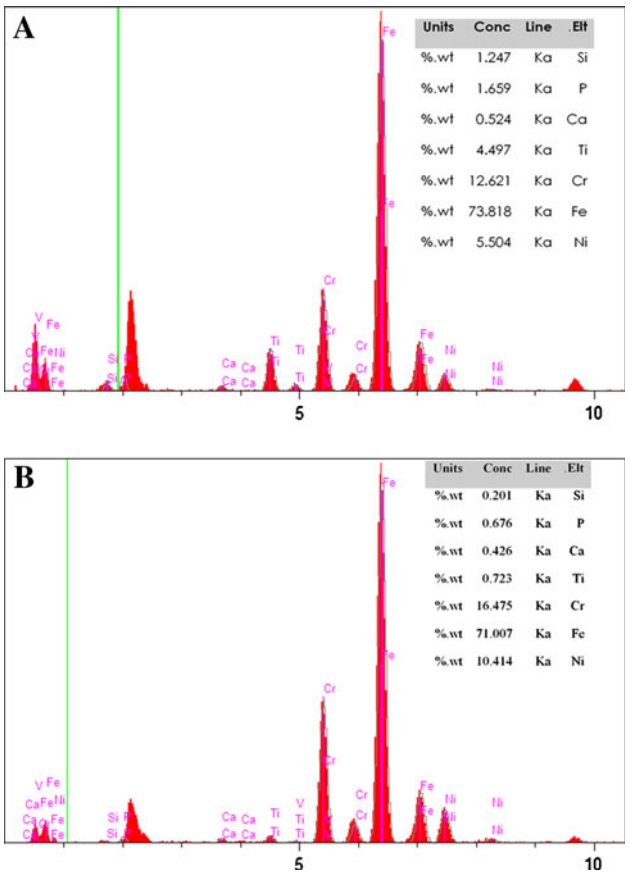

Fig. 9 EDS analysis for (**a**) calcinated NBG-titania film (**b**) Non calcinated NBG-titania films. Fe and Ni picks were obtained from substrate

Table 2 Vickers micro hardness test results for NBG-Titania films

Sample	Vickers hardness numbers	Load (g)	Error values
Calcinated NBG-titania film	358.7	15.15	±10
Non calcinated NBG-titania film	291.5	15.15	±10

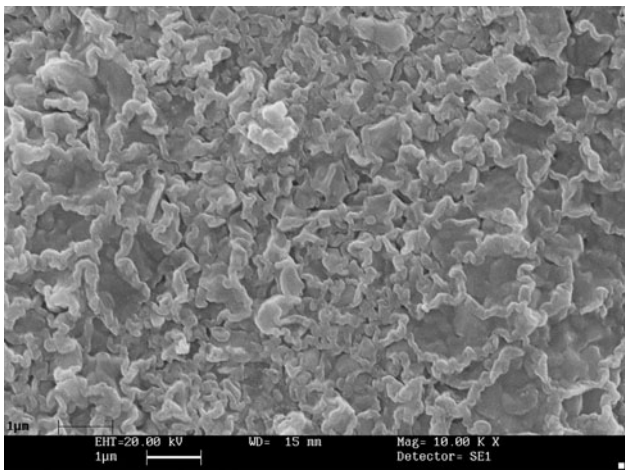

Fig. 10 Dense structure and morphology of calcinated NBG-titania films

Table 3 Vickers micro hardness for some biomedical materials

Materials	Vickers hardness numbers
Alumina	2000–3000
Glass beads	500–550
Bioglass 45S5	458 ± 9.4
Bioglass 58S (Sol–gel derived)	110
Apatite/Wollastonite Bioglass	680
Polycarbonate resin	40–50

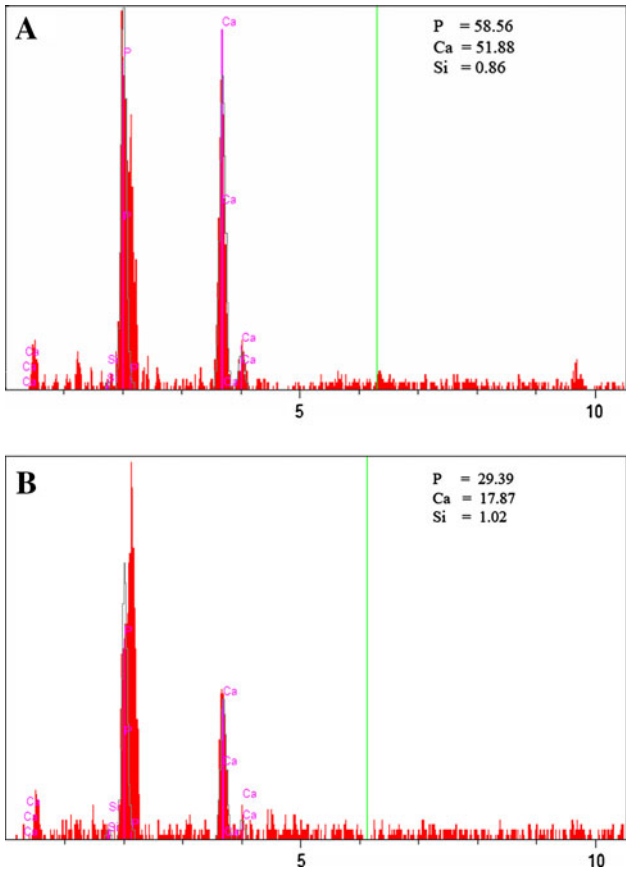

Fig. 11 Electron diffraction spectroscopy (EDS) of apatite formed on (**a**) Calcinated NBG-titania films and (**b**) Non calcinated NBG-titania films after soaking 30 days in SBF

4 Conclusions

In this research, a novel NBG-titania composite film was successfully prepared on 316 L disks using a sol–gel route. Our goal was to study the Influence of calcinated and non calcinated NBG particles on mechanical properties and bioactivity of sol–gel-derived NBG-Titania composite films. The major findings of this study are presented below:

1. The surface analyses showed that the as prepared films with both calcinated and non calcinated NBG particles were all well crystallized, dense and homogeneous

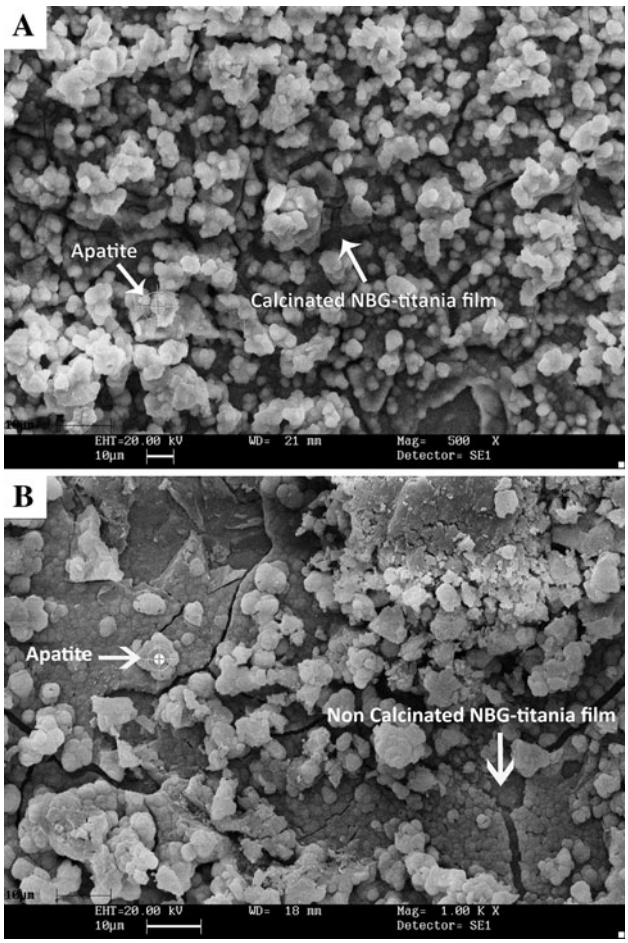

Fig. 12 Scanning electron micrograph of apatite formed on (**a**) calcinated NBG-titania films and (**b**) Non calcinated NBG-titania films after soaking 30 days in SBF

with some submicron pores and cracks due to small residual compressive stresses.

2. SEM and XRD investigations revealed that the films obtained from calcinated NBG particles are thicker than those obtained from non calcinated NBG particles due to higher adhesive properties.
3. The Microhardness tests indicated that calcinated NBG-titania films have a higher hardness than non calcinated NBG-titania films.
4. Bioactivity measurement confirmed that calcinated NBG-titania films have better bioactivity than non calcinated NBG-titania films due to presence of Si–O–Si bands on their surface and also their porous morphology. Also we confirmed that the use of 58S bioglass as a filler agent with titania matrix could increase its bioactivity since in real condition very little amount of HCA can form on the 58S surface even after 4 weeks emersion.

Regarding to above results we can concluded that calcinated NBG-titania films have better Mechanical and bioactivity properties than non calcinated NBG-titania films. Therefore, calcinated NBG-titania coating on stainless steel could be a good substrate in contact with living tissues.

References

1. Hench LL, Spinter RJ, Allen WC, Greenlee TK Jr. Bonding mechanisms at the interface of ceramic prosthetic materials. J Biomed Mater Res. 1971;2(1):117–41.
2. Hench LL. Bioceramics: from concept to clinic. J Am Ceram Soc. 1991;74(1):1487–510.
3. Williams DF. The biocompatibility and clinical uses of calcium phosphate ceramics. In: Williams DF, editor. Biocompatibility of tissue analogs, vol. 2. Boca Raton: CRC Press; 1985. p. 43–66.
4. Hulbert SF, Bokros JC, Hench LL, Wilson J, Heimke G. In: Vincenzini P, editor. Ceramics in clinical applications: past, present and future in high tech ceramics. Amsterdam: Elsevier; 1987. p. 189–213.
5. Le Geros RZ. Calcium phosphate materials in restorative dentistry: a review. Adv Dent Res. 1988;2:164–80.
6. Yamamuro T, Shikata J, Okumura H, Nakamura T, Yoshii S, Ono K, Kitsugi T. Clinical application of bioactive ceramics in bioceramics. Kitsugi Ishiyaku EuroAmerica, Tokio. 1989;1:175–80.
7. Cook SD, Thomas KA. Hydroxya apatite-coated metal for orthopaedic and dental implant applications. Abstracts of the 92nd Annual Meeting and Exposition. The American Ceramic Society, Inc., Dallas, TX. 1990.
8. Yamamuro T, Shikata J, Okumura H, Yoshii S, Konati S, Kokubo T, Heimke G. Pre-clinical and clinical applications of A/W glass–ceramic to various orthopaedic conditions in bioceramics, vol. 2. Cologne: German Ceramic Society; 1990. p. 361–6.
9. De Groot K. Medical applications of calcium phosphate bioceramics. Centennia l Mem Issue. 1991;0.99(10):943–53.
10. Hench LL, Wilson JW. Surface-active biomaterials. Science. 1984;226:630–6.
11. Hench LL. Bioactive glasses and glass–ceramics: a perspective. In: Yamamuro T, Hench LL, Wilson J, editors. Handbook of bioactive ceramics, vol. 1. Boca Raton: CRC Press; 1990. p. 7–23.
12. Ishizawa H, Fujino M, Ogino M. Surface reactions of calcium phosphate ceramics and glass–ceramics to various physiological solutions. In: Yamamuro T, Hench LL, Wilson J, editors. Handbook of bioactive ceramics, vol. 1. Boca Raton: CRC Press; 1990. p. 115–23.
13. Ohtsuki C, Aoki Y, Kokubo T, Bando Y, Neo M, Yamamuro T, Nakamura T. Characterization of apatite layer formed on bioactive glass–ceramic A–W. Bioceramics. 1992;5:79–83.
14. Ohtsuki C, Aoki Y, Kokubo T, Bando Y, Neo M, Yamamuro T, Yacamura T. Characterization of apatite layer formed on bioactive glass–ceramic A–W. Bioceramics. 1992;5:87–94.
15. Ohtsuki C, Kokubo T, Yamamuro T. Mechanism of apatite formation on $CaO–SiO_2–P_2O_5$ glasses in simulated body fluid. J Non-Cryst Solids. 1992;143:84–92.
16. Walker M. An Investigation into the bonding mechanism of bioglass, Doctoral Tesis, Universidad de Florida, 1977.
17. Kokubo T, Hayashi T, Sakka S, Kitsugi T, Yamamuro T. Bonding between bioactive glass, glass–ceramic or ceramics in simulated body fluid. Yogyo-Ky okai-shi. 1987;0.95(8):785–91.
18. Ebisawa T, Kokubo T, Ohura K, Yamamuro T. Bioactivity of $CaO_2·SiO_2$-based glasses: in vitro evaluation. J Mater Sci Mater Med. 1990;1:239–44.

19. Boyde A, Manconnachie E, Muller-Mai C. Gross U.SEM study of surface alterations of bioactive glass and glass-ceramics in bony implantation bed. Clin Mater. 1990;5:73–88.
20. De Aza PN, Guitian F, Merlos A, Lora-Tamayo E, De Aza S. Bioceramics-simulated body fluid interfaces: pH and its influence on hydroxyapatite formation. J Mater Sci Mater Med. 1996;7: 399–402.
21. Sepulveda P, Jones JR, Hench LL. Bioactive sol–gel foams for tissue repair. J Biomed Mater Res. 2002;59:340–8.
22. Yuron C, Lian Z. Effect of thermal treatment on the microstructure and mechanical properties of gel-derived bioglasses. J Mater Chem Phys. 2005;94:283–7.
23. Li J, Sun Y, Sun X, Qiao J. Mechanical and corrosion-resistance performance of electrodeposited titania–nickel nanocomposite coatings. J Surf Coat Technol. 2005;192:331–5.
24. Li P, Kangasniemi I, De Groot K. In vitro and in vivo evaluation of bioactivity of gel titania. Bioceramics. 1993;6:41–5.
25. Haddow DB, James PF, Van Noort R. Characterisation of sol–gel surfaces for biomedical applications. J Mater Sci: Mater Med. 1996;7:255–60.
26. Haddow DB, Kothari S, James PF, Short RD, Hatton PV, Van Noort R. Synthetic implant surfaces. 1. The formation and characterisation of sol–gel titania films. Biomaterials. 1996;17:501–7.
27. Tengvall P, Lundström I. Physico–chemical considerations of titanium as a biomaterial. Clin Mater. 1992;9:115–34.
28. Miyaji F, Zang X, Yao T, Kokubo T, Ohtsuki C, Kitsugi T, Yamamuro T, Nakamura T. Chemical treatment of Ti metal to induce its bioactivity. Bioceramics. 1994;7:119–24.
29. Eckert KL, Ha SW, Mathey M, Wintermantel E. Ceramic processing of titania for biomedical applications. Bioceramics. 1995; 8:447–52.
30. Yan WQ, Nakamura T, Kobayashi M, Kokubo T, Kim HM, Miyaji F. Bone-bonding behavior of titanium implants prepared via chemical treatments. Bioceramics. 1996;9:305–9.
31. Brinker CJ, Hurd AJ, Frye GC, Schunk PR, Ashley CS. In: Hench LL, West JK, editors. Sol-gel thin-film formation in chemical processing of advanced materials. New York: Wiley; 1992. p. 395–413.
32. Sakka S. Preparation and properties of sol-gel coating films. J Sol–Gel Sci Tech. 1994;2:451–5.
33. Zhong J, Greenspan DC. Processing and properties of sol–gel bioactive glasses. J Biomed Mater Res. 2000;53:694.
34. Sepulveda P, Jones JR, Hench LL. In vitro disso- lution of melt-derived 45S5 and sol–gel derived 58S bioactive glasses. J Biomed Mater Res. 2002;61:301.
35. Bielby RC, Christodoulou IS, Pryce RS, Radford WJP, Hench LL, Polak JM. Time- and concentration-dependent effects of dissolution products of 58S sol-gel bioactive glass on proliferation and differentiation of murine and human osteoblasts. Tissue Eng. 2004;10:1018.
36. Kokubo T, Kushitani H, Sakka S, Kitshugi T, Yamamuro T. Solutions able to reproduce in vivo surface-structure changes in bioactive glass-ceramics A-W3. J Biomed Mater Res. 1990;28: 721.
37. Webster TJ, Ergun C, Doremus RH, Siegel RW, Bizios R. Specific proteins mediate enhanced osteoblast adhesion on nanophase ceramics. J Biomed Mater Res. 2000;51:475.
38. Webster TJ, Ergun C, Doremus RH, Siegel RW, Bizios R. Enhanced osteoclast-like cell functions on nanophase ceramics. Biomaterials. 2001;22:1327.
39. Akin FA, Zreiqat H, Jordan S, et al. Preparation and analysis of macroporous TiO_2 on Ti surfaces for bone-tissue implants. J Biomed Mater Res. 2001;57:588.
40. Yerokhin AL, Nie X, Leyland A, et al. Plasma electrolysis for surface. Surf. Coat Technol. 1999;122:73.
41. Duran A, Serna C, Fornes V, Fernandez Navarro JMJ. Structural considerations about SiO_2 glasses prepared by sol–gel. Non Cryst Solids. 1986;82(1–3):69–77.
42. Dutoit DCM, Schmeider M, Baiker A. Titania–silica mixed oxides I Influence of sol–gel and drying conditions on structural properties. J Catal. 1995;153(1):165–76.
43. Zhang M, Shi L, Shuai Y, Zhao Y, Fang J. A novel route to prepare Ph and temperature-sensitive nanogels via a semibatch process. J Colloid Interface Sci. 2009;330(2):113–8.
44. Li R, Clark AE, Hench LL. An investigation of bioactive glass powders by sol–gel processing. J Appl Biomater. 1991;2:231–9.
45. Vallet-Regi M, Izquierdo-Barba I, Salinas AJ. Influence of P_2O_5 on crystallinity of apatite formed in vitro on surface of bioactive glasses. J Biomed Mater Res. 1999;46:560–5.
46. Peltola T, Jokinen M, Rahiala H, Levanen E, Rosenholm JB, Kangasniemi I, Yli-Urpo A. Calcium phosphate formation on porous sol–gel derived SiO_2 and $CaO–P_2O_5–SiO_2$ substrates in vitro. J Biomed Mater Res. 1999;44:12–21.
47. Izquierdo-Barba I, Salinas AJ, Vallet-Regi M. Effect of the continuous solution exchange on in vitro reactivity of a $CaO–SiO_2$ sol–gel glass. J Biomed Mater Res. 2000;51:191–9.
48. Xynos I, Edgar A, Buttery L, Hench L, Polak J. Gene-expression profiling of human osteoblasts following treatment with the ionic products of bioglass 45S5 dissoultion. J Biomed Mater Res. 2001;55:151.
49. Orignac X, Vasconcelos HC, Du XM, Almeida RM. Influence of solvent concentration on the microstructure of $SiO_2–TiO_2$ sol-gel films. J Sol-Gel Sci Technol. 1997;8:243–8.
50. Torruellas WE, Weller Brophy LA, Zanoni R, Stegeman GI, Osborne Z, Zelinski BJJ. Thir-harmonic generation measurement of nonlinearities in $SiO_2–TiO_2$ sol-gel films. Appl Phys Lett. 1991;58:1128–30.
51. Atik M, Zarzycki J. Protective $TiO_2–SiO_2$ coatings on stainless steel sheets prepared by a dip-coating technique. J Mater Sci Lett. 1994;13:1301–4.
52. Almeida RM, Christensen EE. Crystallization behavior of $SiO_2–TiO_2$ sol-gel thin films. J Sol-Gel Sci Technol. 1997;8:409–13.
53. Salama SN, El-Batal HA. Microhardness of phosphate glasses. J Non Cryst Solids. 1994;168:179–85.
54. Coreno J, Rodriguez R, Araiza MA, Castano VM. Growth of calcium phosphate onto coagulated silica prepared by using modified simulated body fluids. J Mater Chem. 1998;8(12):2807–12.